Proceedings of the 21st ICSMGE, Vienna, Austria, 14 – 19 June 2026. Pistrol, Adam & Schweiger (eds.)
Published by: ÖGG, Austrian Society for Geomechanics, Salzburg, Austria, ISBN 978-3-9503898-4-5
https://doi.org/10.53243/ICSMGE2026-675

A novel multilayered soil consolidation solution based on the Spectral method to predict long-term settlement

Bin-Hua Xu, Buddhima Indraratna, Cholachat Rujikiatkamjorn
Transport Research Centre, University of Technology Sydney, Sydney, Australia, binhua.xu@uts.edu.au

Rohan Walker
Maxwell GeoSystems, Kelowna, British Columbia, Canada

ABSTRACT: The consolidation of soft soils is a critical consideration for infrastructure stability, particularly in coastal regions where soft ground typically comprises multiple layers with varying properties. Creep plays a significant role in consolidation and is essential for accurately predicting long-term settlement in viscous soils. Accurate settlement prediction is influenced by loading patterns, soil stratification, and drainage boundary conditions. Despite advancements in theoretical approaches, comprehensive analytical solutions that integrate the effects of multilayered soil profiles and general drainage boundaries remain limited. This study presents a general spectral-based method for analysing the consolidation behaviour of multilayered soils under various loading patterns and drainage boundary conditions, including scenarios with or without prefabricated vertical drains (PVDs), impeded drainage, and time-dependent drainage conditions. The spectral-based solutions employ matrix operations to express the excess pore water pressure (EPWP) as unified solutions across multiple soil layers, effectively capturing the effects of complex boundary conditions. Based on this framework, a simplified Hypothesis B method is proposed to calculate long-term consolidation settlement. The proposed methods are validated against previous analytical solutions for special cases and field data, demonstrating their accuracy and flexibility in predicting EPWP dissipation and settlement. The study provides a more realistic representation of consolidation behaviour by incorporating general drainage conditions expressed as Robin Boundary Conditions (RBCs). The findings offer practical insights for optimizing engineering designs and improving settlement prediction in layered viscous soil foundations, offering a versatile and robust tool for geotechnical engineers to address the complexities of multilayered soil systems under diverse loading and drainage conditions.

KEYWORDS: Consolidation, creep, multilayered soil, spectral method, drainage boundary conditions.

1 INTRODUCTION

The long-term settlement of soft soils remains a central concern in geotechnical engineering, particularly for infrastructure constructed in coastal regions, where the foundation strata often comprise multiple clay layers with varied compressible and hydraulic properties (Xu et al. 2020, 2022, Indraratna et al. 2022, 2024). If not properly assessed and mitigated, excessive post-construction settlements can impair serviceability, cause differential movement, and ultimately compromise the safety of overlying structures (Jiang et al. 2017, 2020, 2024, Xu et al. 2019, 2025a, He et al. 2020, Zhang et al. 2020). Therefore, reliable prediction of consolidation and long-term settlement is crucial to the design and maintenance of transport infrastructure, port facilities, and reclamation projects.

The consolidation process in soft soils involves the dissipation of excess pore water pressure (EPWP) and time-dependent soil settlement. While classical consolidation theories, such as Terzaghi (1925)'s one-dimensional model, have been widely used, their assumptions (such as soil homogeneity, instant loading, and perfectly drained or undrained boundaries) often diverge from actual field conditions. In reality, loads are frequently applied in stages, boundary layers exhibit partial drainage capacity, and soft clay strata are layered with varying compressibility and permeability. Furthermore, conventional models often neglect the contribution of creep, or strain-rate effect, leading to underestimated long-term settlements. This is particularly problematic in soft, viscous clays that exhibit significant time-dependent deformation (Yin and Feng 2017, Baral et al. 2019).

Recent studies have tackled parts of this complexity through analytical models that account for staged loading, spatially variable soil properties, and partially drained boundaries (Lei et al. 2015, Chen et al. 2023). The spectral method has also emerged as an efficient and accurate approach, using global basis functions to handle complex boundary conditions and overcome the eigenvalue limitations of classical methods, especially for multilayered systems (Walker et al. 2009, Walker and Indraratna 2009, 2015, Xu et al. 2021b, 2021a, Nguyen et al. 2022, Xu et al. 2023, 2024, 2025b).

However, a practical gap remains: few analytical or semi-analytical models can simultaneously handle multilayered soil profiles, time-dependent loading, generalized drainage BCs, and long-term settlement prediction. To address this gap, this study develops a general spectral-based consolidation solution in which EPWP dissipation is expressed through matrix-based spectral formulations accommodating arbitrary drainage Boundary Conditions (BCs). Based on this foundation, a simplified Hypothesis B method is incorporated to predict long-term consolidation settlement, capturing creep behaviour through an empirical correction equation. This approach treats creep and consolidation as coupled but separable processes, providing both computational efficiency and physical realism.

The proposed model is validated through comparisons with previous analytical solutions for special cases and field monitoring data. It demonstrates improved accuracy in predicting EPWP dissipation and long-term settlement, especially in systems involving layered soft clays. The findings provide new insights into the interplay between drainage boundaries, soil structure, and time-dependent deformation, offering a robust and practical framework for engineers dealing with complex foundation conditions.

2 THEORETICAL DERIVATION FOR CONSOLIDATION EQUATIONS

2.1 *Governing equations*

Figures 1(a) and (b) illustrate the configurations of multilayered soil systems without and with vertical drains (PVDs), respectively. In the absence of PVD, the consolidation development is controlled only by one-dimensional vertical drainage, and the governing equation accounting for depth-dependent soil properties is expressed as (Xu et al. 2025b):

$$m_v\left(\frac{\partial u}{\partial t}-\frac{\partial Q}{\partial t}\right)=\frac{\partial}{\partial x}\left(\frac{k_v}{\gamma_w}\frac{\partial u}{\partial x}\right) \quad (1)$$

where x and t are the spatial and temporal coordinates, respectively; m_v is the coefficient of volume compressibility; k_v denotes the vertical permeability of the soil; γ_w is the unit weight of the water; Q is the increase in total stress, which can be expressed as $Q(Z,t)=F_s(Z)p(t)$, $p(t)$ represents the variation of external load, $F_s(Z)$ is the vertical total stress distribution; and u is the excess pore water pressure.

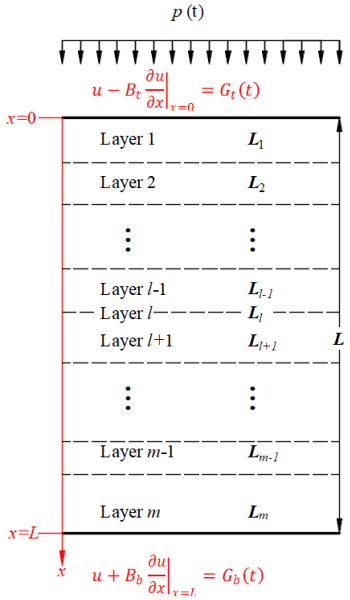

(a) Without PVD

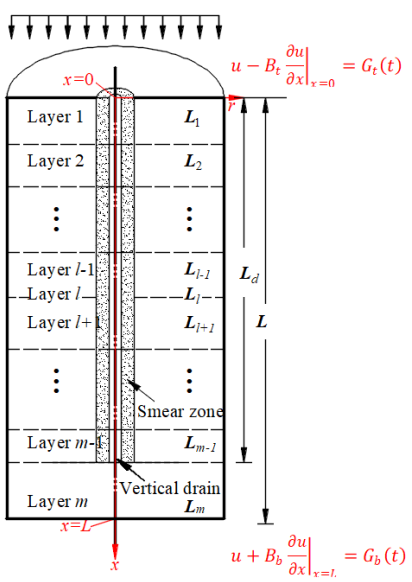

(b) With PVD

Figure 1. Illustration of the multilayered soil system.

When PVDs are installed, both vertical and radial drainage paths contribute to the EPWP dissipation. In this case, the consolidation behaviour is governed by a coupled equation incorporating vertical-radial flow components, considering the variation of soil and drainage properties (Xu et al. 2021b):

$$m_v\left(\frac{\partial u}{\partial t}-\frac{\partial Q}{\partial t}\right)=\frac{\partial}{\partial x}\left(\frac{k_v}{\gamma_w}\frac{\partial u}{\partial x}\right)-\frac{2k_h\left(u-u_w\right)}{\mu r_e^2\gamma_w} \quad (2a)$$

$$\frac{2k_h\left(u_w-u\right)}{\mu r_e^2\gamma_w}=\frac{1}{\gamma_w\left(n^2-1\right)\pi r_w^2}\frac{\partial}{\partial x}\left(q_w\frac{\partial u_w}{\partial x}\right) \quad (2b)$$

where u_w is the prescribed EPWP in the drain, k_h is the undisturbed horizontal permeability, μ is the drain parameter associated with smear and radial geometry, q_w is the drain discharge capacity, r_w and r_e are the drain radius and influence radius, respectively. n is the ratio between r_e and r_w.

2.2 *Boundary conditions*

2.2.1 *Vertical drainage boundary conditions*

In order to express the more realistic representation of the top and bottom BSs corresponding to various situations in real engineering, the general form of Robin Boundary Conditions (RBCs) is adopted as follows (as shown in Fig. 1):

$$u-B_t\frac{\partial u}{\partial x}\Big|_{x=0}=G_t(t) \quad \text{For the top boundary} \quad (3)$$

$$u+B_b\frac{\partial u}{\partial x}\Big|_{x=L}=G_b(t) \quad \text{For the bottom boundary} \quad (4)$$

From the above general form of BCs, it can be seen that the general form of RBCs can represent fully pervious and impervious, semi-permeable and time-dependent drainage BCs.

2.2.2 *Radial drainage boundary conditions*

For the cases with PVDs, the radial drainage BCs are required to solve the governing equations. Based on the equal strain assumption, the average EPWP is used as the variable in the governing equation and the radial BCs are:

$$u\big|_{r=r_w}=u_w \quad (5)$$

$$\frac{\partial u}{\partial r}\Big|_{r=r_e}=0 \quad (6)$$

Based on the above radial BCs, several cases are explained in the following: (i) For the ideal PVDs, where the EPWP in the interface between the drain and the soil is 0, the radial drainage boundary condition can be described as $u|_{r=r_w}=u_w=0$. In this case, Eqs (2a) and (2b) degenerate into the radial consolidation governing equation of ideal drain without considering well resistance. (ii) For the constant discharge capacity (permeability) of the PVDs, the radial drainage BC can be described as $u|_{r=r_w}=u_w|_{r=r_w}\neq 0$, and the value of q_w is constant. (iii) For the reduction of discharge capacity of PVD, which is induced by some field factors (such as bending, clogging, and biodegradation), the radial BCs can be described as $u|_{r=r_w}=u_w|_{r=r_w}\neq 0$, in which the value of $q_w=q_w(Z,t)$.

2.3 *Continuity conditions at the soil interface*

For the multilayered soil system, the continuity conditions of EPWP and flow rate at the soil interface should be satisfied:

$$u^l\big|_{x=L_l}=u^{l+1}\big|_{x=L_{l+1}} \quad (7)$$

$$k_v^l\frac{\partial u^l}{\partial x}\Big|_{x=L_l}=k_v^{l+1}\frac{\partial u^{l+1}}{\partial x}\Big|_{x=L_l} \quad (8)$$

where the superscript l denotes parameters in the l^{th} layer.

2.4 *General solutions based on the Spectral method*

2.4.1 *Geometric and coordinate transformation*

To derive general solutions for the consolidation of multilayered soil systems under general RBCs, this study adopts a geometric and coordinate transformation approach to facilitate the spectral-based formulation. In this method, a

virtual impeded drainage layer is introduced either at the top or bottom (or both) of the multilayered soil system. Subsequently, the vertical coordinate is transformed into a normalized relative depth $Z=\left(x+L_t\right)/H$ to enable efficient solution procedures.

The thicknesses of the virtual drainage layers are determined based on the RBCs described in Eqs. (3)-(4). A practical strategy is to assign the permeability of the virtual layer (assumed rigid and incompressible, i.e., $m_v=0$) to be the same as the permeability at the boundary of the soft clay. Under this assumption, the equivalent thicknesses of the top and bottom virtual layers can be calculated as $L_t=B_t$ and $L_b=B_b$, respectively. Through this transformation, the RBCs can be equivalently converted into Dirichlet BCs, e.g., $u\big|_{Z=0}=G_t(t)$ and $u\big|_{Z=1}=G_b(t)$, as illustrated in Fig. 2. It should be noted that the introduction of a virtual drainage layer allows the model to simulate semi-permeable boundaries. The formulation and eigenvalues of the basis functions corresponding to BCs will be introduced in the following sections.

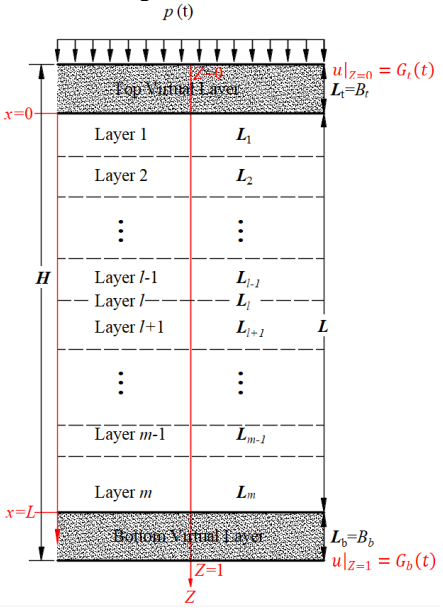

Figure 2. Illustration of the geometric and coordinate transformation of the multilayered soil system.

2.4.2 *Homogenization of nonhomogeneous BCs*

Following the geometric and coordinate transformations, this study applies a homogenization technique to address the nonhomogeneous BCs. In this context, the EPWP variables u and u_w are decomposed as follows:

$$u(Z,t)=\tilde{u}(Z,t)+W(Z,t) \tag{9}$$

$$u_w(Z,t)=\tilde{u}_w(Z,t)+W(Z,t) \tag{10}$$

where $W(Z,t)=(1-Z)G_t(t)+ZG_b(t)$.

By substituting Eq. (9) into Eq. (1), the governing equation for the 1D condition is obtained as Eq. (11), whereas substituting Eqs. (9) and (10) into Eqs. (2a)–(2b) results in the governing equations for the PVD case, given in Eqs. (12a)–(12b).

$$m_v\frac{\partial\tilde{u}}{\partial t}=\frac{1}{\gamma_w H^2}\frac{\partial}{\partial Z}\left(k_v\frac{\partial\tilde{u}}{\partial Z}\right)+\frac{G_b(t)-G_t(t)}{\gamma_w H^2}\frac{\partial k_v}{\partial Z}+m_v\left[F_s(Z)\frac{\partial p(t)}{\partial t}-(1-Z)\frac{\partial G_t(t)}{\partial t}-Z\frac{\partial G_b(t)}{\partial t}\right] \tag{11}$$

$$m_v\frac{\partial\tilde{u}}{\partial t}=\frac{1}{\gamma_w H^2}\frac{\partial}{\partial Z}\left(k_v\frac{\partial\tilde{u}}{\partial Z}\right)+m_v\left[F_s(Z)\frac{\partial p(t)}{\partial t}-(1-Z)\frac{\partial G_t(t)}{\partial t}-Z\frac{\partial G_b(t)}{\partial t}\right] \tag{12a}$$

$$+\frac{G_b(t)-G_t(t)}{\gamma_w H^2}\frac{\partial k_v}{\partial Z}-\frac{2k_h}{\mu r_e^2\gamma_w}\left(\tilde{u}-\tilde{u}_w\right)$$

$$\frac{2k_h}{\mu r_e^2\gamma_w}\left(\tilde{u}_w-\tilde{u}\right)-\frac{\left[G_b(t)-G_t(t)\right]}{\gamma_w\left(n^2-1\right)H^2\pi r_w^2}\frac{\partial q_w}{\partial Z}=\frac{1}{\gamma_w\left(n^2-1\right)H^2\pi r_w^2}\frac{\partial}{\partial Z}\left(q_w\frac{\partial\tilde{u}_w}{\partial Z}\right) \tag{12b}$$

The BCs for the above system are:

$$\tilde{u}(Z,t)\big|_{Z=0}=\tilde{u}_w(Z,t)\big|_{Z=0}=0 \tag{13}$$

$$\tilde{u}(Z,t)\big|_{Z=1}=\tilde{u}_w(Z,t)\big|_{Z=1}=0 \tag{14}$$

2.4.3 *Solutions by using the Spectral method*

Using the spectral method, the variables in the governing equations for both the soft clay and the virtual layers are approximated by truncated series of N terms:

$$\tilde{u}(Z,t)\approx\sum_{j=1}^{N}\Phi_j(Z)A_j(t)=\boldsymbol{\Phi A} \tag{15}$$

$$\tilde{u}_w(Z,t)\approx\sum_{j=1}^{N}\Phi_j(Z)B_j(t)=\boldsymbol{\Phi B} \tag{16}$$

where Φ_j is a set of independent basis functions, and A_j and B_j are expansion coefficients which can vary with time, and

$$\Phi=\left[\Phi_1\ \Phi_2\ \cdots\ \Phi_N\right] \tag{17}$$

$$\mathrm{A}^T=\left[A_1\ A_2\ \cdots\ A_N\right] \tag{18}$$

$$B^T=\left[B_1\ B_2\ \cdots\ B_N\right] \tag{19}$$

Based on the zero BCs in Eqs. (13)-(14), trigonometric functions can be selected as the appropriate basis functions:

$$\Phi_j(Z)=\sin\left(M_jZ\right) \tag{20}$$

The eigenvalues are $M_j=\pi(2j-1)/2$ for an impervious BCs, and $M_j=j\pi$ otherwise,ensuring all BCs are satisfied.

Substituting Eq. (15) into Eq. (11) and applying the spectral method yields the matrix form of the 1D equation:

$$\boldsymbol{\Gamma}\frac{\partial\boldsymbol{A}}{\partial t}+\boldsymbol{\psi A}=\boldsymbol{\theta^k}\left[G_b(t)-G_t(t)\right]+\boldsymbol{\theta}^b\frac{\partial G_b(t)}{\partial t}+\boldsymbol{\theta^Q}\frac{\partial p(t)}{\partial t}+\boldsymbol{\theta}^t\frac{\partial G_t(t)}{\partial t} \tag{21}$$

Similarly, substituting Eqs. (15)–(16) into Eqs. (12a)–(12b) gives the PVD case in matrix form:

$$\boldsymbol{\Gamma}\frac{\partial\boldsymbol{A}}{\partial t}+\left[\boldsymbol{\psi}+\boldsymbol{\zeta}-\boldsymbol{\zeta}(\boldsymbol{\zeta}+\boldsymbol{\chi})^{-1}\boldsymbol{\zeta}\right]\boldsymbol{A}=\boldsymbol{\theta^Q}\frac{\partial p(t)}{\partial t}+\boldsymbol{\theta}^t\frac{\partial G_t(t)}{\partial t}+\boldsymbol{\theta}^b\frac{\partial G_b(t)}{\partial t}+\left[\boldsymbol{\theta^k}+\boldsymbol{\zeta}(\boldsymbol{\zeta}+\boldsymbol{\chi})^{-1}\boldsymbol{\theta^w}\right]\left[G_b(t)-G_t(t)\right] \tag{22}$$

where the elements of matrices $\boldsymbol{\Gamma}$, $\boldsymbol{\theta^t}$ and $\boldsymbol{\theta^b}$ incorporate the compressibility distribution of soft clay; the elements of

matrices $\boldsymbol{\theta}^{\boldsymbol{Q}}$ are related to the combined effect of compressibility and total stress distribution; the elements of matrices $\boldsymbol{\psi}$ and $\boldsymbol{\theta}^{\boldsymbol{k}}$ are related to the vertical permeability distribution of soft soil and virtual layers; the elements of matrices $\boldsymbol{\zeta}$ are related to the vertical distribution of the horizontal permeability; the elements of matrices $\boldsymbol{\theta}^{\boldsymbol{w}}$ and $\boldsymbol{\chi}$ are related to the discharge capacity of vertical drain. The detailed expressions of these elements refer to Xu et al. (2021b, 2025).

Using the method of variation of parameters, $\boldsymbol{A}(t)$ can be obtained as shown in Eq. (21) for the 1D condition, where τ represents a variable of integration (dummy variable):

$$\boldsymbol{A}(t)=e^{-\int_0^t \boldsymbol{\Gamma}^{-1}\boldsymbol{\psi}d\tau}\times \left\{\int_0^t e^{\int_{-\infty}^{\tau}\boldsymbol{\Gamma}^{-1}\boldsymbol{\psi}ds}\boldsymbol{\Gamma}^{-1}\begin{bmatrix}\boldsymbol{\theta}^{\boldsymbol{Q}}\dfrac{\partial p(\tau)}{\partial\tau}+\boldsymbol{\theta}^{t}\dfrac{\partial G_t(\tau)}{\partial\tau}\\ +\boldsymbol{\theta}^{b}\dfrac{\partial G_b(\tau)}{\partial\tau}+\boldsymbol{\theta}^{\boldsymbol{k}}G_b(\tau)\\ -\boldsymbol{\theta}^{\boldsymbol{k}}G_t(\tau)\end{bmatrix}d\tau\right\} \tag{23}$$

Following the same way and defining $\boldsymbol{\Omega}=\boldsymbol{\psi}+\boldsymbol{\zeta}-\boldsymbol{\zeta}(\boldsymbol{\zeta}+\boldsymbol{\chi})^{-1}\boldsymbol{\zeta}$, $\boldsymbol{A}(t)$ can be obtained as shown in Eq.(22) for the case with PVD can be obtained:

$$\boldsymbol{A}(t)=e^{-\int_0^t \boldsymbol{\Gamma}^{-1}\boldsymbol{\Omega}d\tau}\times \left\{\int_0^t e^{\int_{-\infty}^{\tau}\boldsymbol{\Gamma}^{-1}\boldsymbol{\Omega}ds}\boldsymbol{\Gamma}^{-1}\begin{bmatrix}\boldsymbol{\theta}^{\boldsymbol{Q}}\dfrac{\partial p(\tau)}{\partial\tau}+\boldsymbol{\theta}^{t}\dfrac{\partial G_t(\tau)}{\partial\tau}\\ +\boldsymbol{\theta}^{b}\dfrac{\partial G_b(\tau)}{\partial\tau}+\boldsymbol{\theta}^{\boldsymbol{k}}G_b(\tau)\\ -\boldsymbol{\theta}^{\boldsymbol{k}}G_t(\tau)+G_b(\tau)\\ -\boldsymbol{\zeta}(\boldsymbol{\zeta}+\boldsymbol{\chi})^{-1}\boldsymbol{\theta}^{\boldsymbol{w}}G_t(\tau)\end{bmatrix}d\tau\right\} \tag{24}$$

Further, the EPWP can be obtained from Eqs. (15) and (16). Then, the DOC based on the settlement for a certainlayer and the overall layers can be obtained by:

$$U_l=\frac{\int_{Z_l}^{Z_{l+1}}m_v(Z)\left(F_s(Z)p(t)-\boldsymbol{\Phi A}(t)\right)dZ}{p_f\int_{Z_l}^{Z_{l+1}}m_v(Z)F_s(Z)dZ} \tag{25}$$

$$U=\frac{\int_0^1 m_v(Z)\left(F_s(Z)p(t)-\boldsymbol{\Phi A}(t)\right)dZ}{p_f\int_0^1 m_v(Z)F_s(Z)dZ} \tag{26}$$

For different loading patterns (ramp, exponential, trigonometric), the solutions can refer to Xu et al. (2025). For the general RBCs and loading patterns, which can be expanded in harmonic components using the Fourier series or combined with some basic patterns, and then a general solution can be obtained, the detailed solutions can refer to Xu et al. (2025).

3 A SIMPLIFIED HYPOTHESIS B METHOD FOR CALCULATING LONG-TERM SETTLEMENT

While the spectral-based consolidation solutions in the previous section effectively capture the consolidation behaviour of multilayered soils under varied drainage and loading conditions, long-term settlement prediction must account for creep. Unlike Hypothesis A, which assumes creep occurs only after EPWP dissipation; Hypothesis B considers that part of the creep deformation develops concurrently with consolidation. This assumption is more realistic for soft clays where structural viscosity and effective stress redistribution evolve continuously during EPWP dissipation. To address this, a simplified Hypothesis B method proposed by Yin et al. (2022) is adopted, in which the total long-term settlement S_t is expressed as:

$$\begin{aligned}S_t&=S_p+S_c=\sum_{l=1}^{l=m}U_lS_{fl}+\sum_{l=1}^{l=m}S_{cl}\\&=U\sum_{l=1}^{l=m}S_{fl}+\sum_{l=1}^{l=m}\left[\alpha U_l^{\beta}S_{c,fl}+\left(1-\alpha U_l^{\beta}\right)S_{c,dl}\right]\end{aligned} \tag{27}$$

where S_p is the separated settlement apart from the creep settlement; S_c the creep settlement; U_l is the average DOC for the l^{th} layer; U is the combined average DOC for all multiple soil layers with or without a PVD; S_{fl} is the final "primary" consolidation settlement at the End-Of-Primary consolidation for the l^{th} layer; S_{cl} is creep settlement of soil skeleton in the l^{th} layer, representing the time-dependent deformation of the soil structure during the consolidation process; $S_{c,fl}$ is creep settlement of the l^{th} layer under the "final" vertical effective stress after load increased, representing the delayed creep deformation that continues after primary consolidation has completed; $S_{c,dl}$ is the "delayed" creep settlement of the l^{th} layer under the "final" vertical effective stress ignoring the EPWP; α is the parameter to reasonably consider the creep compression coupled with consolidation; β is a power index with value from 0 to 1. It is noted that $S_{c,dl}$ will be zero for $t\le t_{EOP,Field}$ and will become positive for $t\ge t_{EOP,Field}$. $C_{\alpha\varepsilon}$ is a creep parameter to calculate the final creep settlement.

For each soil layer (l^{th} layer), the final "primary" consolidation settlement S_{fl} is computed by using volume compressibility m_v or Cc and C_r; it is noted that the parameters m_v or Cc and C_r and pre-consolidation stress are all determined from the standard oedometer test with duration of 24 h for each load and for each layer. The details about the calculation of $S_{c,fl}$ and $S_{c,dl}$ can be found in Yin et al. (2022).

4 VERIFICATION AND APPLICATIONS

4.1 *Verification against existing analytical solutions for special cases*

To validate the accuracy and applicability of the proposed comprehensive consolidation model, comparisons were made with existing analytical solutions for specific boundary and loading conditions.

(1) Impeded drainage boundaries

Liu and Ma (2013) developed an analytical solution for 1D consolidation with impeded drainage boundaries under ramp loading, capable of capturing the effect of partial drainage layers and a linearly varying stress distribution with depth. When $G_t(t) = G_b(t) = 0$, $B_t = L_t$, $B_b = L_b$, the proposed model simplifies to Liu and Ma's formulation. The soil properties and geometrical parameters are $L = 10$ m, $H = 16$ m, $k_v(Z) = 2.00\times10^{-9}$ m/s, $L_t = 4L$, $L_b = 2L$, $m_v(Z) = 6.60\times10^{-4}$ m^2/kN. The applied load is ramp loading, the loading stage is 100 d, and the stress distribution is $F_s(Z) = 1 - 0.9Z$. The dimensionless time factor $T_v = k_v^1 t \Big/ m_v^1\gamma_w L^2$ is used in this study.

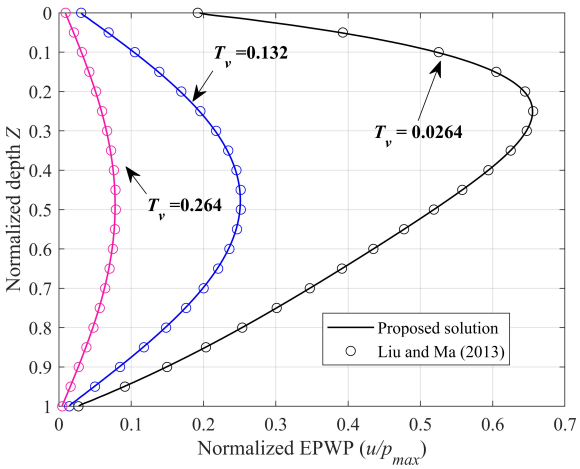

Figure 3. Comparison of the proposed solutions and analytical solutions under impeded drainage conditions.

It can be seen from Fig. 3 that the normalized excess pore water pressure (EPWP) distributions at different time predicted by the proposed model match Liu and Ma (2013)'s solution closely, confirming its capability to handle impeded drainage conditions and depth-dependent stress profiles.

(2) Continuous drainage boundaries and various loading types

Chen et al. (2022) presented a multilayered analytical solution for consolidation under continuous drainage boundaries and various loading types. When $B_t(t) = B_b(t) = 0$, $G_t(t) = p_{max}e^{-bt}$ and $G_b(t) = p_{max}e^{-ct}$, the proposed model simplifies to the solutions by Chen et al. (2022). The four-layered soils are analysed, the BCs parameters are $b = 15.67$, $c = 156700$, and the soil parameters can be seen in Table 1. The results demonstrate excellent agreement between the two models for the entire consolidation process, confirming the proposed model's robustness for multilayer soil profiles, continuous drainage boundaries, and complex loading scenarios, as shown in Fig. 4.

Table 1. Parameters of the four-layered soils (Chen et al. 2022).

Layer No.	H_i (m)	k_v (10^{-6} m/d)	E_s (MPa)
1	3.05	2.402	15.50
2	6.10	7.128	24.47
3	9.15	1.011	49.44
4	6.10	2.540	24.69

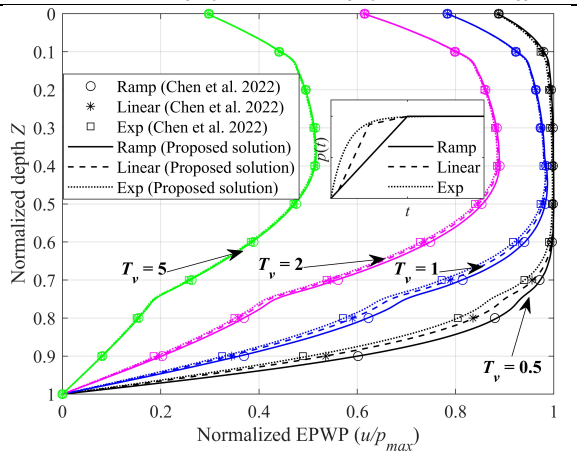

Figure 4. Comparison of the proposed solutions and analytical solutions under continuous drainage boundaries and various loading.

4.2 *Case study-Lilla Mellösa Test Site*

To demonstrate the practical applicability of the proposed model, a case study was conducted using field data from the Lilla Mellösa test site in Sweden. The site consists of layered clays, overlain by a partially permeable topsoil layer and underlain by a highly permeable bottom layer. A 2.5 m high fill of gravel with a density of 1.7 t/m^3 was constructed for 25 days and kept the same during the test. The model incorporated soil parameters (Table 2) and realistic BCs: partially permeable drainage at the top and fully permeable drainage at the bottom. For the long-term settlement calculation, the creep parameter $C_{\alpha\varepsilon} = 0.0376$, $\alpha = 0.2$.

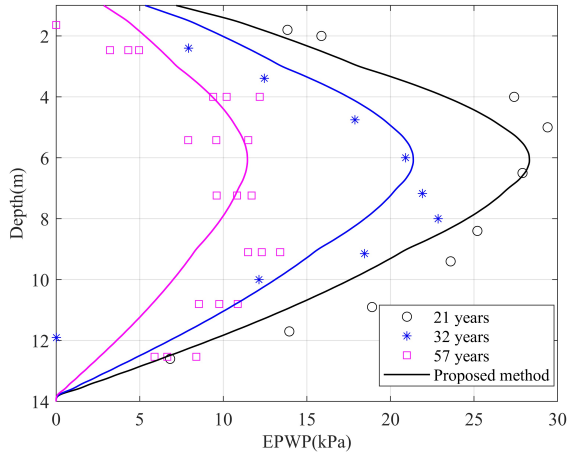

(a) EPWP

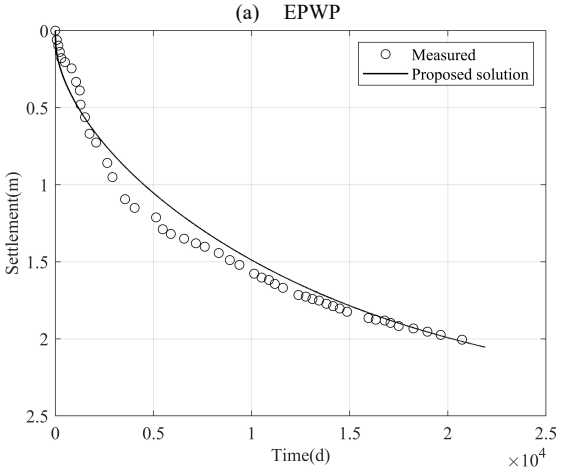

(b) Settlement

Figure 5. Comparison of the proposed solutions and measured data.

Table 2. Soil properties used in Lilla Mellösa test site (Hansbo 2005).

Depth (m)	Description	$\Delta\sigma_v$ (kPa)	E_s (kPa)	k (m/year)
0-1	Topsoil, dry crust	42	9000	0.02
1-1.5	Green organic clay, shell	42	200	0.02
1.5-3	Dark grey organic clay, shell	41	200	0.025
3-5	Black/dark grey organic clay, shell	41	190	0.018
5-7	Dark grey clay	40	160	0.015
7-9	Grey clay	39	240	0.022
9-11	Grey varved clay	38	280	0.03
11-14	Grey varved clay	33	200	0.03

The simulated EPWP dissipation along depth and settlements at different times are shown in Fig. 5, which compares closely with field measurements (Larsson and Mattsson 2003), particularly in capturing the slower pore pressure dissipation near the top layer. The results highlight the importance of correctly accounting for partial drainage boundaries and creep in predicting consolidation behaviour and confirm the proposed model's applicability for real-world engineering problems.

5 CONCLUSIONS

A spectral-based solution is developed for consolidation analysis of multilayered soils under general drainage boundaries and time-dependent loading. Using geometric coordinate transformation and virtual drainage layers, the method converts RBCs to an equivalent Dirichlet form, enabling efficient computation with global trigonometric functions. While the spectral method offers high accuracy and efficiency compared with conventional finite-difference formulations, its reliance on smooth property variation may reduce performance for highly discontinuous soil profiles. Verification against existing analytical solutions and field data demonstrates high accuracy in predicting EPWP dissipation and settlement, including creep effects. The approach provides a practical tool for complex soft soil foundation design and performance assessment.

6 ACKNOWLEDGEMENTS

The Authors also acknowledge the support from the Transport Research Centre (TRC), University of Technology Sydney. This research is also sponsored by the Australian Research Council (ARC) Discovery Project (DP230101769) and Linkage Project (LP230100199).

7 REFERENCES

Baral, P., Rujikiatkamjorn, C., Indraratna, B., Leroueil, S., and Yin, J.-H. 2019. Radial Consolidation Analysis Using Delayed Consolidation Approach. Journal of Geotechnical and Geoenvironmental Engineering, **145**(10): 04019063.

Chen, H.X., Feng, S.J., Zhu, Z.W., Gao, L., Chen, Z.L., and Wang, S.R. 2023. One-dimensional self-weight consolidation of layered soil under variable load and semi-permeable boundary condition. Computers and Geotechnics, **159**: 105431.

Chen, X., Chen, W., and Yue, Z. 2022. One-dimensional consolidation of multilayered soil with continuous drainage boundaries and under time-dependent loading. International Journal of Geomechanics, **22**(9): 04022142(1–10).

Hansbo, S. 2005. Experience of Consolidation Process from Test Areas with and without Vertical Drains. Ground Improvement Case Histories: Embankments with Special Reference to Consolidation and Other Physical Methods,: 33–82.

He, B., He, N., Xu, B.-H., Cai, R., Shao, H.-L., and Zhang, Q.-L. 2020. Tests on distributed monitoring of deflection of concrete faces of CFRDs. Yantu Gongcheng Xuebao/Chinese Journal of Geotechnical Engineering, **42**(5).

Indraratna, B., Sai, R., Nair, L., and Rujikiatkamjorn, C. 2024. Instrumentation and Data Interpretation in Transportation Geotechnics. Indian Geotechnical Journal, **54**(1): 40–62.

Indraratna, B., Singh, M., Nguyen, T.T., Rujikiatkamjorn, C., Malisetty, R.S., Arivalagan, J., and Nair, L. 2022. Internal Instability and Fluidisation of Subgrade Soil under Cyclic Loading. Indian Geotechnical Journal, **52**(5): 1226–1243.

Jiang, Y.-B., He, N., Xu, B.-H., Zhou, Y.-Z., and Zhang, Z.-L. 2017. Model tests on negative pressure distribution in vacuum preloading. Yantu Gongcheng Xuebao/Chinese Journal of Geotechnical Engineering, **39**(10).

Jiang, Y., He, N., Zhou, Y., Xu, B., Zhan, X., and Ding, Y. 2020. Investigation on in situ test and measurement technique of groundwater level in vacuum preloading. Bulletin of Engineering Geology and the Environment, **79**(3).

Jiang, Y., Li, S., He, N., Xu, B., and Fan, W. 2024. Centrifuge Modeling Investigation of Geosynthetic- Reinforced and Pile-Supported Embankments. International Journal of Geomechanicschanics, **24**(8): 04024147.

Larsson, R., and Mattsson, H. 2003. Settlements and shear strength increase below embankments. : 1–98.

Lei, G.H., Zheng, Q., Ng, C.W.W., Chiu, A.C.F., and Xu, B. 2015. An analytical solution for consolidation with vertical drains under multi-ramp loading. Géotechnique, **65**(7): 531–541.

Liu, J.-C., and Ma, Q. 2013. One-Dimensional Consolidation of Soft Ground with Impeded Boundaries Under Depth-Dependent Ramp Load. *In* First International Symposium on Pavement and Geotechnical Engineering for Transportation Infrastructure. Nanchang, China. pp. 127–134.

Nguyen, T.T., Indraratna, B., Rujikiatkamjorn, C., and Xu, B.-H. 2022. Evaluation on the performance of field embankment testing biodegradable drains based on spectral method analysis. *In* Proceedings of 20th International Conference on Soil Mechanics and Geotechnical Engineering (ICSMGE 2022). Sydney, Australia. pp. 3031–3036.

Terzaghi, K. 1925. Erdbaumechanik auf bodenphysikalischer grundlage. Vienna: Leipzig Deuticke.

Walker, R., and Indraratna, B. 2009. Consolidation analysis of a stratified soil with vertical and horizontal drainage using the spectral method. Géotechnique, **59**(5): 439–449.

Walker, R., Indraratna, B., and Sivakugan, N. 2009. Vertical and radial consolidation analysis of multilayered soil using the spectral method. Journal of Geotechnical and Geoenvironmental Engineering, **135**(5): 657–663.

Walker, R.T.R., and Indraratna, B. 2015. Application of spectral Galerkin method for multilayer consolidation of soft soils stabilised by vertical drains or stone columns. Computers and Geotechnics, **69**: 529–539. Elsevier Ltd.

Xu, B.-H., He, N., Jiang, Y.-B., Zhou, Y.-Z., and Zhan, X.-J. 2020. Experimental study on the clogging effect of dredged fill surrounding the PVD under vacuum preloading. Geotextiles and Geomembranes, **48**(5): 614–624.

Xu, B.-H., He, N., Zhou, Y.-Z., and Zhang, Z.-L. 2021a. Nonlinear consolidation model of stratified soil with vertical drains based on the spectral method. Yantu Gongcheng Xuebao/Chinese Journal of Geotechnical Engineering, **43**(10): 1781–1788.

Xu, B.-H., Indraratna, B., Carter, J.P., Rujikiatkamjorn, C., and Kelly, R. 2025a. A theoretical framework to describe undrained yielding and potential fluidisation of soft subgrade soil under cyclic loading. Géotechnique, **In press**.

Xu, B.-H., Indraratna, B., Nguyen, T.T., and Walker, R. 2021b. A vertical and radial consolidation analysis incorporating drain degradation based on the spectral method. Computers and Geotechnics, **129**: 103862.

Xu, B.-H., Indraratna, B., Rujikiatkamjorn, C., and Nguyen, T.T. 2022. A large-strain radial consolidation model incorporating soil destructuration and isotache concept. Computers and Geotechnics, **147**: 104761.

Xu, B.-H., Indraratna, B., Rujikiatkamjorn, C., Nguyen, T.T., and He, N. 2023. Nonlinear consolidation analysis of multilayered soil with coupled vertical-radial drainage using the spectral method. Acta Geotechnica, **18**: 1841–1861.

Xu, B.-H., Indraratna, B., Rujikiatkamjorn, C., Yin, J.-H., Kelly, R., and Jiang, Y.-B. 2025b. Consolidation analysis of inhomogeneous soil subjected to varied loading under impeded drainage based on the spectral method. Canadian Geotechnical Journal, **62**: 1–21.

Xu, B., He, N., and Li, D. 2019. Study on the treatments and countermeasures for liquefiable foundation. *In* MATEC Web of Conferences. p. 01012.

Xu, B.H., Indraratna, B., Rujikiatkamjorn, C., He, N., and Nguyen, T.T. 2024. Spectral-Based Solutions for Consolidation Analysis of Multilayered Soil under Various Drainage Boundary Conditions. *In* Proceedings of the 5th International Conference on Transportation Geotechnics (ICTG) 2024, Volume 4: Applied Ground Improvement Methods. pp. 17–28.

Yin, J., Chen, Z., and Feng, W.-Q. 2022. A general simple method for calculating consolidation settlements of layered clayey soils with vertical drains under staged loadings. Acta Geotechnica, **2**.

Yin, J.H., and Feng, W.Q. 2017. A new simplified method and its verification for calculation of consolidation settlement of a clayey soil with creep. Canadian Geotechnical Journal, **54**(3): 333–347.

Zhang, Z., He, N., He, B., Xu, B., and Jiang, Y. 2020. New method to measure structure stress based on distributed optical fiber technology. Chinese Journal of Scientific Instrument, (9): 45–55.